

Crystal Plasticity Analysis of Thermal Deformation and Dislocation Accumulation in ULSI Cells

Michihiro Sato^{1, a}, Tetsuya Ohashi^{1, b}, Takuya Maruizumi² and Isao Kitagawa³

¹Department of Mechanical Engineering, Kitami Institute of Technology,
165 Koen-cho, Kitami, Hokkaido 090-8507 Japan

²Department of Electrical and Electronic Engineering, Musashi Institute of Technology,
1-28-1 Tamazutsumi, Setagaya-ku, Tokyo 158-8557, Japan

³Advanced Research Laboratory, Hitachi, Ltd.,
1-280 Higashi-koigakubo, Kokubunji, Tokyo 185-8601, Japan

^asato@newton.mech.kitami-it.ac.jp, ^bohashi@newton.mech.kitami-it.ac.jp,

Keywords : ULSI, Dislocation, Crystal plasticity analysis, Finite element method

Abstract. Thermal stress, plastic slip deformation and accumulation of dislocations in shallow trench isolation (STI) type ULSI devices when the temperature drops from 1000 to room temperature are analyzed by a crystal plasticity analysis code. The results show that dislocation accumulation takes place at the temperature range over 800, and the difference of 6 MPa in the lattice friction stress at 1000 causes increase of dislocation density more than 1.6 times. Dislocations generate and accumulate at the shoulder part of the device area and bottom corners of the trench. Dislocations are categorized into two groups. In one group, dislocation lines are mostly straight and parallel to the trench direction, and in the other group, dislocations make half loop type structure. Possibilities for the suppression of dislocation accumulation through control of lattice friction stress at high temperature region are discussed.

Introduction

In recent years, high-density memories and high-speed CPUs are usually realized by a reduction of the size of semiconductor cells in LSIs. Representative length scale of ULSI cells is going to be at a nano-meter order and the atomic level defects, such as uneven oxidation film or lattice defect generation etc., are becoming more and more important. Among them, dislocations which often appear near hetero-interfaces and accumulate in the electron channel have an enormous effect on the electronic state of the device, increase the signal delay and obstruct devices from normal operation. Therefore, the evaluation and control of dislocations are crucial not only for the design of cell structure but also for the design of process through which ULSI chips are produced. The periodic structure of the shallow trench isolation (STI) type ULSI cells are generally adopted as the latest semiconductor device structure. A lot of investigations have been made on this type of structure and dislocation accumulation is known to be caused by thermo-plastic deformation in silicon during the processes of device fabrication, but detailed aspects on dislocations and their density distribution in the cells are not fully understood. In this study, we analyse such thermal stress, plastic slip deformation and accumulation of dislocations in STI type ULSI devices when the temperature drops from 1000 to room temperature. For the analyses, we use a continuum mechanics based crystal plasticity analysis code CLP[1,2].

Model for numerical analysis

Fig. 1 (a) schematically shows the periodic structure of the STI type ULSI cells. One unit of the periodic structure is cut out and we employ it for the numerical analyses. Fig. 1 (b) shows the model used in the analyses. Dimensions of the model is typical for STI structure with the gate length 62 nm. The structure consists of the volumes to , as shown in Fig. 1 (b). Volumes

to corresponds to gate, source and drain electrodes, respectively, and for simplicity their materials are assumed to be SiO₂. Volume represents the Si substrate. Crystal orientation of the model is also shown in Fig. 1 (b). The normal of Si substrate (the Y axis) corresponds to the [100] direction and trench direction of STI structure is parallel to the [011] direction. Table 1 shows the material data [3,4] used for the analysis. We assume the deformation in the z direction is negligibly small because the dimension of the STI structure in the z direction is long enough compared to those in the x and the y direction. Then, in the numerical model, the nodes on the surfaces perpendicular to the z axis are constrained to displace in the z direction. Nodes on the surfaces which are perpendicular to the x axis are subjected to obey a periodic boundary condition in the x direction. The models are divided into finite elements. The type of the elements is the composite element with eight nodes. The numbers of nodes and elements in a model is 4446 and 2812, respectively.

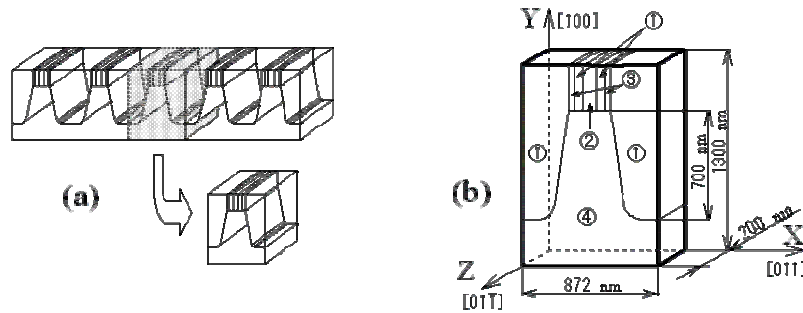


Fig. 1 (a) Schematic illustration of the periodic structure of the STI type ULSI cells.
(b) Model employed for the crystal plasticity analysis.

Table 1 Material data used in the analyses [3,4].

	Elastic compliances [10 ⁻¹¹ m ² /N]			Thermal expansion coefficient [1/K]
Si	S ₁₁ =0.7685	S ₁₂ =-0.2139	S ₄₄ =1.2563	2.50 × 10 ⁻⁶
SiO ₂	S ₁₁ =1.3698	S ₁₂ =-0.2327	S ₄₄ =3.2051	0.35 × 10 ⁻⁶

Numerical analysis

The CLP analyzes the plastic slip deformation on 12 slip systems of {111}<110> and evaluates the plastic shear strains, stresses and the density distributions of geometrically necessary (GN) dislocations. The critical resolved shear stress on slip system is given by the modified Bailey-Hirsch type relation;

$$\theta^{(n)} = \theta_0(T) + \sum_{m=1}^{12} \Omega^{(nm)} a \mu \tilde{b} \sqrt{\rho_s^{(m)}}. \quad (1)$$

Where, the first term of the right hand side of Eq. 1 gives the lattice friction stress and the second term denote the strain hardening. For simplicity, we assume a sufficiently small value for a and exclude the effect of strain hardening. Therefore, the critical resolved shear stresses on slip systems are decided only by temperature and do not depend on deformation history. As far as we know, there is no experimental data of lattice friction stress. On the other hand, the hardness of silicon was experimentally obtained in the range from 24 to 800 (Table 2), where hardness values are normalized by the hardness at 800 . It is known, in general, that plastic flow stress is proportional to the hardness of crystalline material. In this paper, we made three data sets P1, P2 and P3 for the lattice friction stress (Fig. 2). One set of data given by the P3 curve shown in Fig. 2 are calculated in such a way that the lattice friction stress at 800 is 30 MPa and vary with temperature in the same way the hardness values H3 change. At temperature lower than 800 , the lattice friction stress increases when the temperature drops as shown by symbols of , and the lattice friction stress at 24 becomes 10.2 times larger than the value at 800 . Similarly,

lattice friction stresses given by the data set P2 are calculated from the hardness with the H2 series of data. P1 is the reference function and the lattice friction stress is constant (30MPa) for any temperature. We assume the lattice friction stress of P1, P2 and P3 is constant at temperature higher than 800 , because there are no data in this temperature range.

Table 2 Hot hardness values for silicon [5].

Temperature []	H2	H3
24	7.9	10.2
100	7.4	9.8
200	7.1	9.3
400	6.2	5.6
600	2.3	2.6
800	0.8	1.0

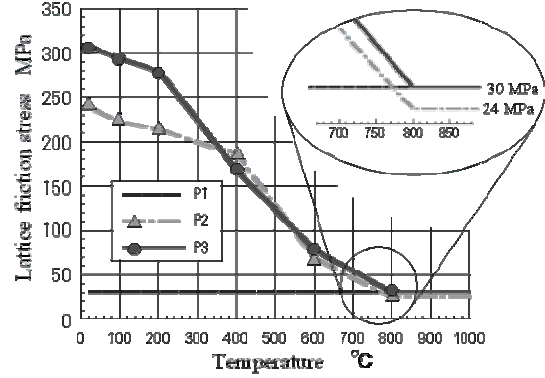


Fig. 2 Lattice friction stress curves used in the analyses.

Results and discussion

Fig. 3 (a) and (b) show numerical results for the density distribution of the geometrically necessary dislocations on the $(111)[\bar{1}\bar{1}0]$ and $(11\bar{1})[\bar{1}\bar{1}0]$ slip systems, when the lattice friction stress is given by the data set P3 and the temperature drops from 1000 to room temperature. Longer and thicker line segments represent higher density of dislocations. Direction of line segments is drawn parallel to the dislocation line. Dislocations accumulated on the $(111)[\bar{1}\bar{1}0]$ slip system and shown in Fig. 3 (a) are mostly straight and lie parallel to the trench direction at the shoulder part of the device area and bottom corner of the trench. Dislocations accumulated on $(111)[10\bar{1}]$, $(\bar{1}\bar{1}\bar{1})[110]$ and $(\bar{1}\bar{1}\bar{1})[101]$ slip systems also make up a similar structure as the one shown in Fig. 3 (a). On the other hand, dislocations shown in Fig. 3 (b) make up half loop shaped structure at bottom corners of the trench and at the shoulder part of the device area. Dislocations on $(11\bar{1})[101]$, $(11\bar{1})[110]$ and $(11\bar{1})[10\bar{1}]$ slip systems also make up a similar structure as the one given in Fig. 3 (b). Therefore, there are two categories in terms of the shape of dislocation accumulation and four slip systems belong to each category. In the following discussions, we focus on dislocations on the $(111)[\bar{1}\bar{1}0]$ and $(11\bar{1})[\bar{1}\bar{1}0]$ slip systems.

We define the total length of dislocations (tdl) on each slip systems by the following equation;

$$\text{tdl}^{(n)} = \sum_i \|\rho_G^{(n)}\| \times v_i. \quad (2)$$

where, ρ_G is the density norm of the geometrically necessary dislocations, v_i is the volume of element i , and superscript (n) denotes the slip system number, respectively. Fig. 4 (a) and (b) show evolution of the tdl, as a function of temperature and lattice friction curves P1, P2 and P3. When the lattice friction stress is given by P1 and have no temperature dependence, the total length of dislocations monotonically increases when the temperature drops. When the lattice friction stress is given by P2, tdl on the $(111)[\bar{1}\bar{1}0]$ slip system starts to increase at 840 and converge at 800 (Fig. 4 (a)). When the lattice friction stress is given by P3, a slight amount of dislocations on the $(111)[\bar{1}\bar{1}0]$ slip system accumulate at 800 but it does not show notable growth. Fig. 4 (b) shows growth of tdl on the $(11\bar{1})[\bar{1}\bar{1}0]$ slip system. When the lattice friction stress is given by P2 and P3, dislocations begin to accumulate at 880 and 860 , respectively and these values converge at 800 . As shown in Fig. 2, difference in the lattice friction stress given by P2 and P3 is 6 MPa in the range from 1000 to 800 . By this small difference of 6 MPa, the temperature at which dislocations start to accumulate differ 40 on the $(111)[\bar{1}\bar{1}0]$ slip system and 20 on the $(11\bar{1})[\bar{1}\bar{1}0]$ slip system. While, the temperature at which dislocation accumulation converge is

800 for both cases. The final values of tdl on the $(11\bar{1})[1\bar{1}0]$ slip system are 1.4×10^{-7} m for P2 case and 8.6×10^{-8} m for P3 case (Fig. 4 (b)). So, the difference of 6 MPa in the lattice friction stress at high temperature caused increase of dislocation accumulation more than 1.6 times. These facts show that the difference of a few MPa in the lattice friction stress at the temperature range from 1000 to 800 is decisive for dislocation accumulation.



Fig. 3 Structures of GN dislocations on the $(111)[1\bar{1}0]$ slip system at 600 (a), and on the $(11\bar{1})[1\bar{1}0]$ slip system at 760 (b).

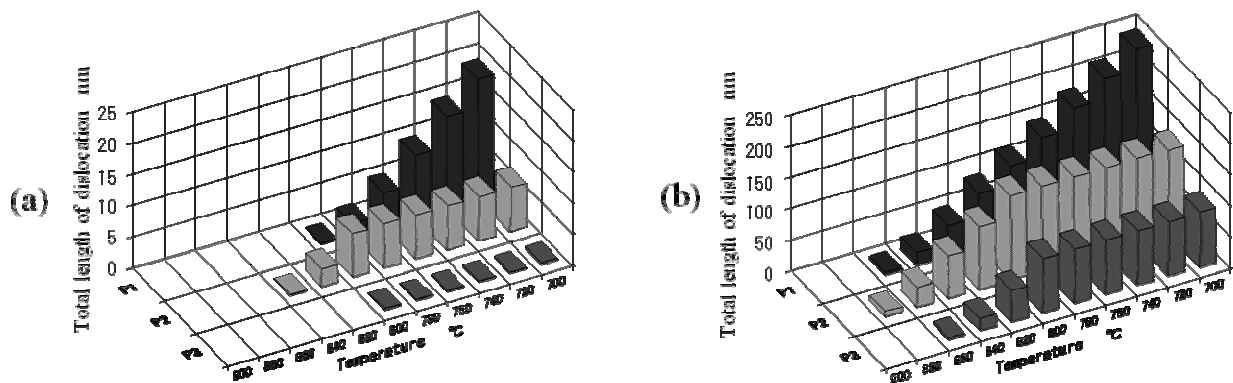


Fig. 4 Total length of dislocations during cooling on the $(111)[1\bar{1}0]$ slip system (a) and on the $(11\bar{1})[1\bar{1}0]$ slip system (b).

Summary

We analyzed thermo plastic deformation and dislocation accumulation in the periodic structure of shallow trench isolation (STI) type ULSI cells when the temperature drops from 1000 to room temperature. Results are summarized as follows;

- (1) Two types structure of dislocations generated at the shoulder part of the device area and bottom corners of the trench when the temperature dropped.
- (2) Dislocation accumulation converged at 800 when the temperature dependency of lattice friction stress was considered, while it grew approximately linearly when the lattice friction stress was assumed to be kept constant.
- (3) It was concluded that control of lattice friction stress at high temperature region is one of promising way for the suppression of dislocation accumulation in STI type ULSIs.

References

- [1] Ohashi, T., *Phil. Mag. Lett.*, 75(1997), 51.
- [2] Ohashi, T., *Int. J. Plasticity*, 21(2005), 2071.
- [3] *Semiconductors Handbook*, revised ed., edited by Semiconductors Handbook Compilation Committee, Ohm-sha Publishing, Tokyo, 1977, p. 135.
- [4] *Encyclopedia for Physics and Chemistry*, 3rd ed., edited by B. Tamamushi, Iwanami Publishing, Tokyo, 1981, pp. 1068,1151.
- [5] Properties of Silicon, EMIS DATA REVIEWS SERIES No.4, AHMED, H. , INSPEC, (1988),22